NASA TECHNICAL MEMORANDUM

NASA TM X-52159

NASA TM X-52159

RADIAL DENSITY AND TEMPERATURE PROFILES AT THE ION CYCLOTRON WAVE RESONANCE POINT

by Roman Krawec
Lewis Research Center
Cleveland, Ohio

TECHNICAL PAPER proposed for presentation at Plasma Dynamics Conference sponsored by the American Institute of Aeronautics and Astronautics Monterey, California, March 2-4, 1966

NATIONAL AERONAUTICS AND SPACE ADMINISTRATION · WASHINGTON, D.C. · 1966

RADIAL DENSITY AND TEMPERATURE PROFILES AT THE ION CYCLOTRON WAVE RESONANCE POINT

by Roman Krawec

Lewis Research Center
Cleveland, Ohio

TECHNICAL PAPER proposed for presentation at

Plasma Dynamics Conference
sponsored by the American Institute of Aeronautics and Astronautics
Monterey, California, March 2-4, 1966

RADIAL DENSITY AND TEMPERATURE PROFILES AT THE ION CYCLOTRON WAVE RESONANCE POINT

by Roman Krawec*

Lewis Research Center

National Aeronautics and Space Administration

Cleveland, Ohio

E-3324

ABSTRACT

A simplified theory for an electrostatic probe in a magnetically confined plasma is presented. Interpretation of probe results using the model are compared with those calculated from Langmuir probe theory. The model presented provides an expression for calculating ion temperature from the probe data. Radial profiles of electron density, radial electric field, electron temperature, and ion temperature are presented for two experiments: (1) a d.c. hot-cathode low-pressure (2μ) discharge confined by a steady magnetic field; and (2) a plasma heating experiment where ion cyclotron waves propagate along the plasma column. The radial electron density profiles show that the maximum density does not occur on axis but at radii of 0.5 to 1.0 cm (the plasma radius was approximately 2.5 cm). The average densities are found to be in agreement with microwave interferometer measurements and consistent with the location of maximum power transfer. The ion and electron temperatures are found to reach a maximum near the plasma boundary. The addition of rf power is found to heat both the ions and electrons but has little effect on the density.

*Aerospace Research Engineer.

TM X-52159

INTRODUCTION

Experiments attempting to relate the amount of rf power absorbed by a magnetically confined plasma to plasma density, plasma radius, coil wavelength, and magnetic field have been carried out at the Lewis Research Center and at other laboratories (a review of these experiments is given in Ref. 1). According to the theory of Stix (Ref. 2), the value of the magnetic field at which maximum power absorption occurs is primarily a function of ion density when the radio frequency is near the ion cyclotron frequency. The amount of power transfer, however, is strongly dependent on the plasma diameter. In Ref. 2 a cylindrical plasma of uniform density and ion temperature was assumed. It has recently been shown (Ref. 3) that the radial density and ion temperature distribution of the plasma will affect both the shape and the magnitude of the resonant peak. It thus becomes apparent that a knowledge of these radial profiles is needed in order that any experiment can properly be compared with theory.

The availability of density and temperature profiles also allows a comparison with a recently developed stability criterion of Roth (private communication) which states that a sufficient condition for stability is that the product of the density and temperature be a constant across a plasma diameter for both the ions and the electrons.

The purpose of this paper is to present these profiles and to compare them with ion cyclotron heating theory and with stability criteria. A new model of an electrostatic probe in a d.c. magnetic field is developed and is used to calculate radial profiles of temperature and density. The results of the calculations are compared with Langmuir probe theory and with microwave measurements where applicable.

THEORY

The following plasma-probe model is set up to obtain the desired density

and temperature profiles. The plasma is considered to be composed of electrons and a single species of ions, and to be contained by a magnetic field. The probe is considered to be of arbitrary shape but of a size such that it is large compared to the gyro radius of the electrons but small compared to the gyro radius of the ions. The ions are thus considered to have an isotropic Maxwellian velocity distribution while the velocity distribution of the electrons is considered to be one-dimensional Maxwellian and parallel to the d.c. magnetic field. Sheath effects are considered to be negligible.

In general, the current through a given area is given by the product of the charge, the charged particle density, and the velocity, integrated over the velocity distribution function. If the probe is below plasma potential, all of the ions will be collected and the integration is performed from zero to infinity. The results of this integration are

$$I_{ri} = n_o q A_i \left[\frac{kT_i}{2\pi M}\right]^{1/2} \tag{1}$$

where I_{ri} is the random ion current, n_o is the ion density (assumed equal to the electron density since the Debye length is typically less than 10^{-4} cm), A_i is the surface area of the probe, T_i is the ion temperature, M is the ion mass, and the other symbols have their usual meanings.

The lower limit of the integration is not zero for the electron current since only those electrons which can overcome the potential barrier existing between the probe and the plasma will be collected. The electron current is thus given by

$$I_e = q n_o A_e \left[\frac{kT_e}{2\pi m}\right]^{1/2} e^{-qV/kT_e} \tag{2}$$

where A_e is the area of the projection of the probe on a plane normal to the magnetic field, T_e is the electron temperature, m is the electron mass, and V is the probe voltage measured with respect to plasma potential. The

random electron current is obtained from the above expression by setting V equal to zero.

The electron temperature may be found by considering the probe to be at floating potential and setting the electron and ion currents equal to each other. After some manipulation, this gives

$$kT_e = qV_f/\ln I_s \tag{3}$$

where

$$I_s = \frac{I_{re}}{I_{ri}} = \frac{A_e}{A_i}\left[\frac{MT_e}{mT_i}\right]^{1/2} \tag{4}$$

Equations (3) and (4) are solved to give the ion temperature as

$$kT_i = \frac{qV_fM}{\ln I_s m}\left[\frac{A_e}{I_sA_i}\right]^2 \tag{5}$$

The density may be found from the random electron current (Eq. (2) with V = 0) and is given by

$$n_o = \frac{2I_{re}}{qA_e}\left[\frac{\pi m \ln I_s}{2qV_f}\right]^{1/2} \tag{6}$$

Thus the electron density, electron temperature, and the ion temperature can be found from a measurement of the floating potential and the two saturation currents.

It might be instructive to compare the above results with expressions frequently used in probe analysis. Eq. (2) may be written as

$$I_e = I_{re}e^{-qV/kT_e}$$

From which

$$\frac{qV}{kT_e} = \ln I_{re} - \ln I_e$$

$$\frac{d}{dV}(\ln I_e) = \frac{-q}{kT_e}$$

This expression is commonly used to obtain the electron temperature from Langmuir probe data and is common to the two models. Eq. (3) however, can be

a much more rapid means of analyzing the experimental data.

Eq. (6) gives the density in terms of the electron and ion saturation currents. The electron saturation current is not normally used when the plasma is immersed in a magnetic field. An approximate formula for charged particle density (also from the usual Langmuir probe theory) in terms of the ion saturation current is given (Ref. 4) by

$$n_{lp} \simeq \frac{I_{ri}}{0.4\ A_i q} \left[\frac{M}{2kT_e}\right]^{1/2} \tag{7}$$

Here the ion saturation current and the electron temperature are used to calculate the number density. A comparison with Eq. (1) shows that Eq. (7) corresponds to Eq. (1) with the quantity $2T_e$ used in place of T_i.

The derivation of Eq. (7) assumes that $T_e \gg T_i$ and that the ion collection is determined by the sheath surrounding the probe. The present expression (Eq. (6)) anticipates plasmas where T_i may be greater than T_e. Comparing the above with Eq. (4) gives:

$$\frac{n_o}{n_{lp}} = .8\ I_s \frac{A_i}{A_e} \left[\frac{\pi m}{M}\right]^{1/2}$$

For a plasma consisting of atomic hydrogen ions and for a cylindrical probe perpendicular to the magnetic field for which $A_i = \pi/2\ A_e$, this expression becomes:

$$\frac{n_o}{n_{lp}} = \frac{I_s}{19.24}$$

Thus the ratio of densities calculated from the two equations will depend only on the ratio of the measured saturation currents.

EXPERIMENTAL APPARATUS

The experimental apparatus used was a continuously operating magnetic mirror machine with a 2:1 mirror ratio. A schematic of one half of the main portion of the vacuum chamber and of the magnetic field configuration is

given in Fig. 1. The chamber is 5 cm in radius and has an aluminum oxide center section with a 4-section Stix type coil around it. The gas feed and the filament structure for the electron bombardment source are located at one end of the chamber while the pumping system is attached to the other end. There was a continuous flow of hydrogen gas that maintained the pressure within the main portion of the vacuum chamber at 2 microns. The overall length of the vacuum chamber is 255 cm. The uniform region of the magnetic field was adjusted to a value of approximately 4500 gauss for the series of measurements reported here. The ion cyclotron wave was excited with a two-wavelength Stix coil operating at a radio frequency of 6.5 Mc. The coil wavelength was 40 cm.

The probe was located at port 1 (Fig. 1) at the end of the apparatus nearest the filament structure. A schematic of the cross section of the vacuum chamber at the probe location and details of probe construction are given in Fig. 2. The probe consisted of a small loop of 0.01 inch diameter tungsten wire which could be heated to the temperature required for electron emission by passing a d.c. current through it. The probe was attached to a hydraulic actuator which was used to move the probe radially into and out of the plasma at a controlled rate. The probe actuator control system provided a voltage output which was proportional to the probe position. All data were taken as a function of radial probe position.

The measurements taken consisted of the floating potential of the cold probe, the floating potential of the emissive probe, the ion saturation current, and the electron saturation current.

It has been pointed out (Ref. 5) that the floating potential of the emissive probe is very nearly the same as the plasma potential. The difference in floating potentials between the hot probe and cold probe thus gives the quantity V_f needed in the equations.

The method of measuring the ion and electron saturation currents is illustrated in Fig. 3 which gives a typical probe trace obtained at a fixed radius. This trace has been drawn so that zero voltage corresponds to zero net current to the probe. The probe was biased to some voltage A which was below the zero net current voltage. The current measured at this point was taken as the ion saturation current and was believed to be no more than ±5% in error.

The electron saturation current was obtained in a similar manner except that the electron current was measured at three voltages above plasma potential (points B, C, and D). These values of current were then extrapolated (with a straight line) to give the current at plasma potential. This method generally gives a value for the electron saturation current which is believed to be as much as 15% too high.

Data were taken on the plasma formed by the electron bombardment discharge alone, and on the plasma formed when both the discharge and the rf transmitter were turned on. For the latter case, the amount of rf power was first measured as a function of magnetic field and the field at which maximum power absorption occurred was determined for the values of discharge current used. Probe measurements were then taken at these maximum power points. Both types of plasma were operated at a steady state.

The values of discharge current used were 10, 15, 20, and 25 amperes; only typical profiles (15 amperes) will be presented here.

RESULTS AND DISCUSSION

The electron density as a function of radius is given in Fig. 4. The error bars indicate the uncertainty in position due to the length of the probe and the estimated errors in measuring saturation currents. The solid curves in this figure represent profiles computed from Eq. (6) while the dotted curves represent profiles computed from the approximate Langmuir probe

relation (Eq. (7)). Although the profiles from the two methods appear quite different, the average of these radial densities turns out to be the same. It thus becomes impossible to decide which is the correct method from a consideration of the average density obtained with a microwave interferometer.

The profiles presented are typical of the four sets of data that were taken. The features of these four sets may be summarized as follows: (1) in general, the maximum density did not always occur on axis but was found at radii of up to 0.75 cm when the rf was off, and at radii of from 0.5 to 1.0 cm when the rf was on. This type of profile has previously been reported (Refs. 6 and 7); (2) the maximum values of density ranged from 2.65 to 7.65×10^{11} electrons per cubic cm when the rf was off, and from 2.1 to 7.4×10^{11} electrons per cubic cm when the rf was on; (3) the average values of density (taken of an area passing through the axis of the vacuum chamber) ranged from 1.15 to 3.13×10^{11} electrons per cubic cm when the rf was off, and from 0.80 to 2.04×10^{11} electrons per cubic cm when the rf was on; and (4) the radius of the plasma at a point corresponding to half the maximum density was 2.17 to 2.25 cm when the rf was off, and 1.12 to 1.83 cm when the rf was on.

The average densities which were presented above are compared with microwave densities in Table 1. The percentage difference between the two methods of measuring the average density was 25.0 to 75.0% when the rf was off, and 0.8 to 22.9% when the rf was on. Thus, the agreement between the probe and the microwave measurements is much better in the presence of rf. This may be attributed to the fact that the quantity V_f is much larger when the rf is on and can thus be more accurately measured.

The radial profile of the electron temperature is presented in Fig. 5. When the rf was off, the electron temperature was approximately 3 ev and did not vary greatly across the plasma radius. This was found to be true for all

four discharge currents. When the rf was turned on, the temperatures varied from 5 to 7.5 ev at the axis and gradually increased to maximum values of from 40 to 66.5 ev at a radius of approximately 3.75 cm.

The ion temperatures (Fig. 6) showed a similar behavior. When the rf was off, the on-axis temperatures were found to be approximately 3 to 5 ev up to a radius of approximately 2 cm, and then increased to 13 to 170 ev. Maximum temperatures cannot be given for these cases since the temperature increases occurred in regions of vanishing plasma density where the currents to the probe became too small to measure. The on-axis temperatures ranged from 1.4 to 16.2 ev when the rf was turned on and rose to peak values of 980 to 1875 ev. Three of the cases considered attained maximum ion temperature at approximately 3.5 cm; the maximum for the fourth case was at 2.2 cm. Figs. 5 and 6 indicate that the temperatures are generally higher when the rf is on. Thus, the addition of rf tends to heat both components of the plasma.

The ion temperatures that have been presented are much higher than expected and this raises the question of whether or not some factor has been neglected in setting up the model. Two such factors have been ignored; (1) the plasma contains an externally generated monoenergetic electron beam, and (2) the plasma is composed of two ion species which may be of different temperatures. If these factors are taken into account, the consequent correction will increase the calculated ion temperature. Thus, the ion temperatures presented herein may be lower than the true ion temperature.

However, the model has obvious defects when one supposes such hot plasmas. For example, a probe in a plasma with $T_i \simeq 10^3$ ev could be expected to emit electrons due to bombardment by such ions. Also, in a low density region the plasma sheath may no longer be a small fraction of the probe diameter, i.e., the values of A_i and A_e may be functions of the

probe position. Obviously, an independent confirmation of these high ion temperatures is desirable.

There are two other plasma properties which may be computed from the data taken. These are the radial electric field and the net charge density. These are obtained by taking the first and second derivative of the plasma potential (Fig. 7) with respect to radius and substituting into the expressions $E_r = -\partial\varphi/\partial r$ and $\rho = \epsilon \nabla^2\varphi$. Only the electric field has been calculated for this paper and is presented in Fig. 8. The electric field is seen to rise towards the plasma boundary for both cases presented. The major difference between the two cases lies in the region between the center of the plasma and the wall. The rf can be seen to give rise to regions of strong fields which are distinguishable from each other by the direction of the field. The mechanism by which an rf magnetic field can give rise to a strong dc electric field is not understood. It should be emphasized that the fields presented here are averages over the probe length (0.4 cm); the true fields may be much larger.

The density and temperature profiles presented may be compared with a proposed stability criterion which states that a sufficient condition for both microscopic and macroscopic plasma stability is that the quantity nkT be a constant in the radial direction for both the ions and the electrons. The products have been formed and are presented in Fig. 9. The stability criterion is quite well satisfied for the central region of the plasma, but not near the plasma edge. This does not mean that the plasma is unstable in this region, since the criterion gives a sufficient condition but not a necessary one.

The knowledge of peak and average densities allows a comparison with the relation given by Stix that specifies the magnetic field strength at the resonant peak in terms of axial and radial wavelength, ion cyclotron

frequency, transmitter frequency, and plasma density. If the axial wavelength is taken as the wavelength of the driving coil, the two extreme values of the radial wavelength may be used to give a density region where the waves can propagate.

The relation becomes, for the two cases

$$\lambda_z^2 = \frac{4\pi^2}{An_e}\left[\frac{1 - \Omega^2}{\Omega^2}\right] \quad \text{for} \quad \lambda_r = 0$$

and

$$\lambda_z^2 = \frac{4\pi^2}{An_e}\left[\frac{1 - \Omega}{\Omega^2}\right] \quad \text{for} \quad \lambda_r = \infty$$

In the above equation, Ω is the ratio of ion cyclotron frequency to the transmitter frequency, λ_z is the axial wavelength, λ_r is the radial wavelength, n_e the electron density (assumed uniform over the plasma radius), and A is a constant. These relations are plotted in Fig. 10 for the two principal axial driving wavelengths present in the experiment. The cross hatched regions represent the particular range of plasma density and Ω for which cyclotron waves of 44.5 and 89 cm axial wavelengths can be propagated. Values of the measured peak and average densities are also plotted. The values of average densities fall along the boundary of the 89 cm existence region while the peak densities fall in the space between existence regions. This suggests that power is coupled to the plasma via the 89 cm wavelength component of the rf coil, and that the plasma responds as if its density were uniform and equal to the average density measured by the microwave interferometer.

CONCLUDING REMARKS

The results of this investigation are as follows:

(1) Equations were obtained which permit calculation of electron and ion temperature and plasma density from measurements of floating potential

and the electron and ion saturation currents in a magnetically confined plasma.

(2) The measurement of the difference in floating potentials (relative to ground) of an emissive probe and a cold probe was found to be a convenient measure of the actual voltage drop across the sheath when the net current is zero.

(3) Measurements of radial density, temperature, and electric field profiles were made for two experiments: (a) a hot-cathode low-pressure hydrogen discharge operated at several discharge currents, and (b) the same discharge operated with the addition of rf power.

(4) The average densities from integrated probe measurements were found to agree within 75% with microwave interferometer measurements.

(5) The average values of the density were found to be in agreement with the theory for generation and propagation of ion cyclotron waves.

REFERENCES

1. Hooke, W. M. and Rothman, M. A., "A Survey of Experiments on Ion Cyclotron Resonance in Plasmas," Nucl. Fusion 4, 33 (1964).

2. Stix, T. H., "Generation and Thermalization of Plasma Waves," Phys. Fluids 1, 308 (1958).

3. Vasil'ev, M. P., Grigor'eva, L. I., Dolgopolov, V. V., Smerdov, B. I., Stepanov, K. N. and Chechkin, V. V., "Cyclotron Resonance in an Inhomogeneous Plasma Cylinder," Soviet Phys.-Tech. Phys. 9, 953 (1965).

4. Glasstone, S. and Lovberg, R. H., "Controlled Thermonuclear Reactions, an Introduction to Theory and Experiment," (D. Van Nostrand Company, Inc., Princeton, 1960).

5. Domitz, S., "Experimental Evaluation of a Direct-Current Low-Pressure Plasma Source," NASA Tech. Note D-1659 (April 1963).

6. Kolb, A. C., Lupton, W. H., Elton, R. C., McLean, E. A., Swartz, M., Young, M. P., Griem, H. R. and Hintz, E., "Plasma Confinement, Heating and Losses in PHAROS with an Extended Current Pulse." Second International Conference on Plasma Physics and Controlled Nuclear Fusion Research, Culham, England, September 6-10, 1965. International Atomic Energy Agency Paper No. CN21/98.

7. Stodiek, W., Grove, D. J. and Kessler, J. O., "Plasma Confinement in Low-Density C Stellarator Discharges." Second International Conference on Plasma Physics and Controlled Nuclear Fusion Research, Culham, England, September 6-10, 1965. International Atomic Energy Agency Paper No. CN21/120.

TABLE I. - COMPARISON OF PROBE AND MICROWAVE MEASUREMENT OF AVERAGE ELECTRON DENSITY

(a) With rf power off

Beam current, A	Probe electron density, n_e, electrons/cm^3	Microwave electron density, n_e, electrons/cm^3	Percent difference[a]
10	1.15×10^{11}	$.92 \times 10^{11}$	25.0
15	1.88×10^{11}	1.50×10^{11}	25.3
20	3.13×10^{11}	1.79×10^{11}	75.0
25	2.79×10^{11}	2.11×10^{11}	32.2

(b) With rf power on

10	$.80 \times 10^{11}$	$.82 \times 10^{11}$	2.4
15	1.30×10^{11}	1.33×10^{11}	1.9
20	2.04×10^{11}	1.66×10^{11}	22.9
25	1.94×10^{11}	1.93×10^{11}	.8

[a] Percent difference $= \dfrac{|\text{Probe } n_e - \text{microwave } n_e|}{\text{Microwave } n_e} \times 100$ percent.

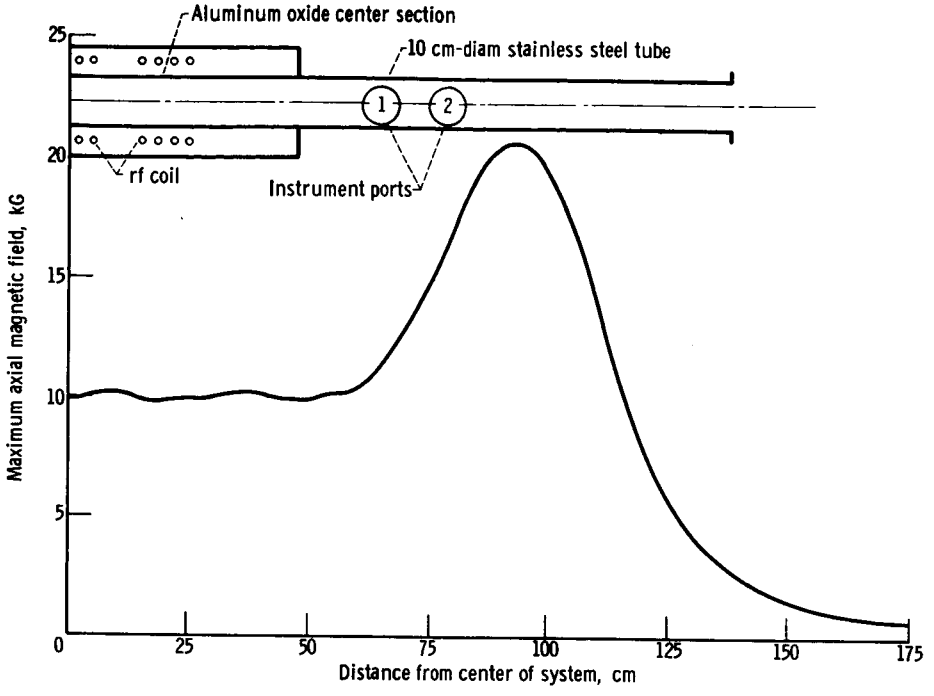

Figure 1. - Magnetic field and vacuum chamber configuration.

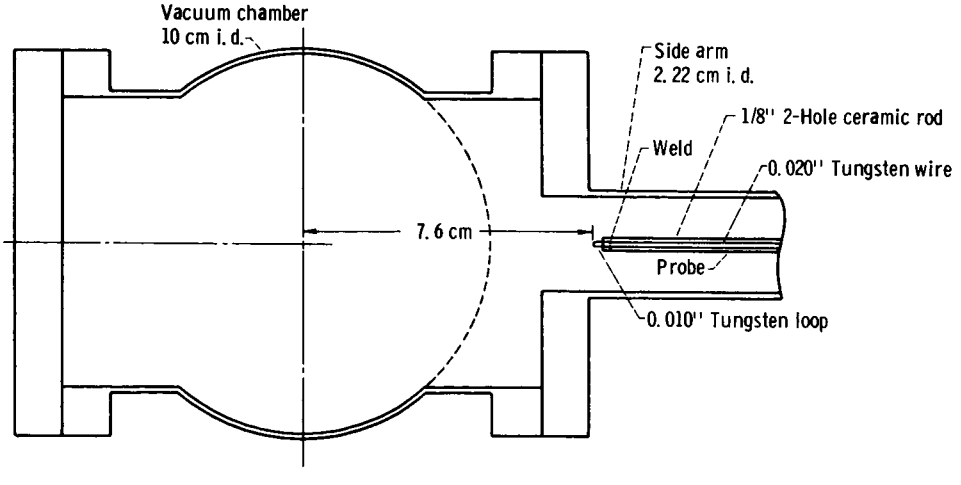

Figure 2. - Schematic of vacuum chamber cross section at probe location and probe details.

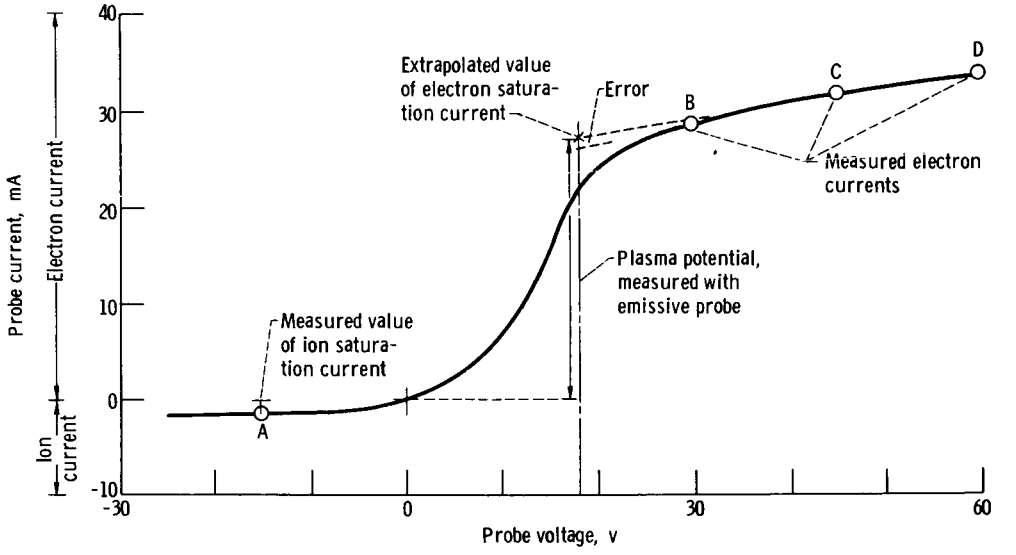

Figure 3. - Typical probe trace showing method of measuring electron and ion saturation currents.

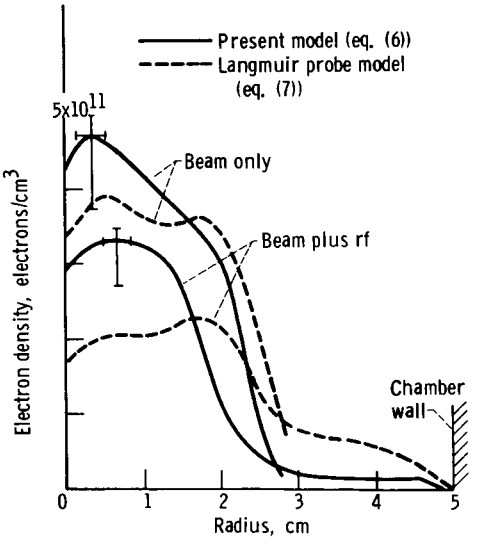

Figure 4. - Electron density profile. Current, 15 A.

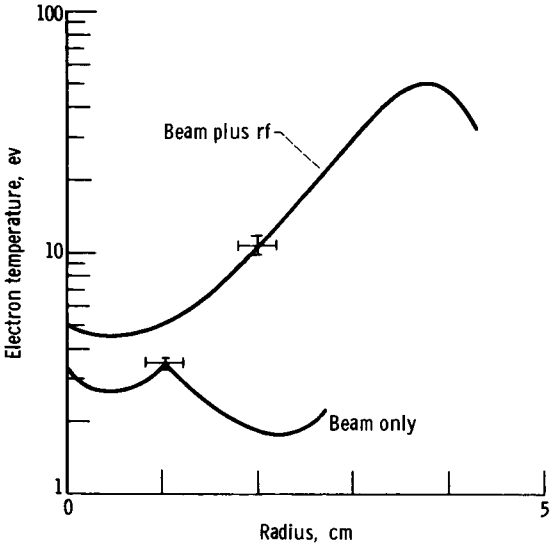

Figure 5. - Electron temperature profile. Current, 15 A.

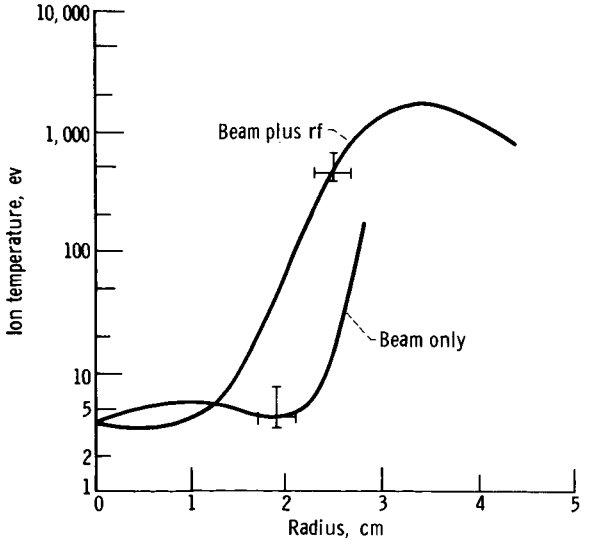

Figure 6. - Ion temperature profile. Current, 15 A.

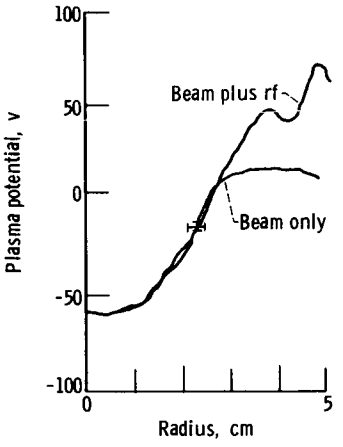

Figure 7. - Plasma potential profile. Current, 15 A.

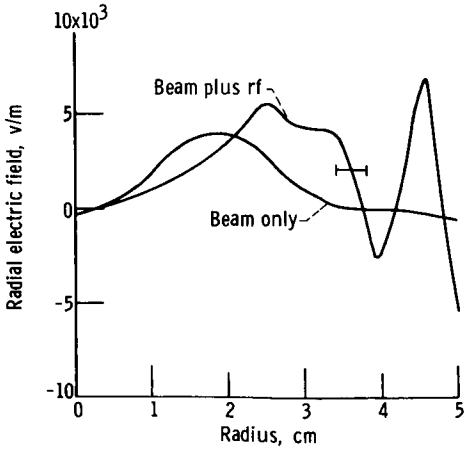

Figure 8. - Radial electric field profile. Current, 15 A.

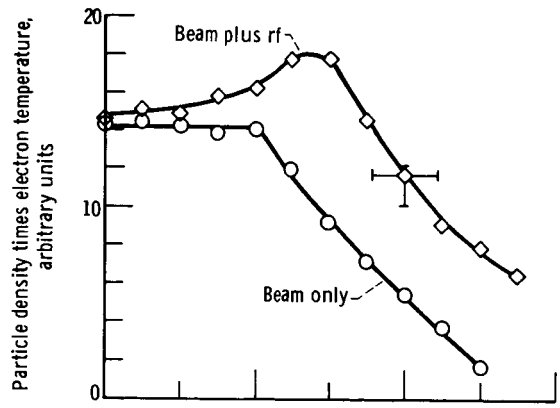

(a) Particle density times electron temperature.

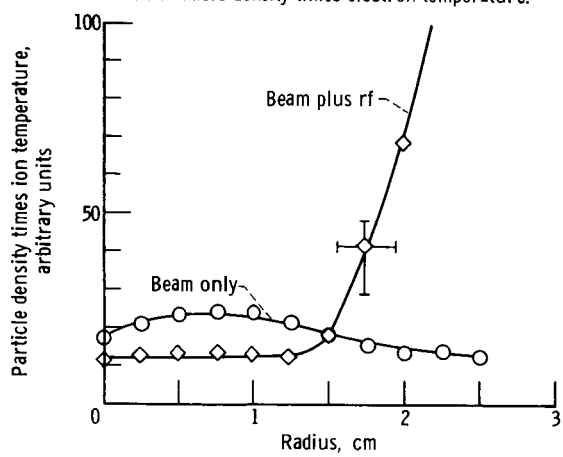

(b) Particle density times ion temperature.

Figure 9. - Application of stability criteria to 15 ampere runs.

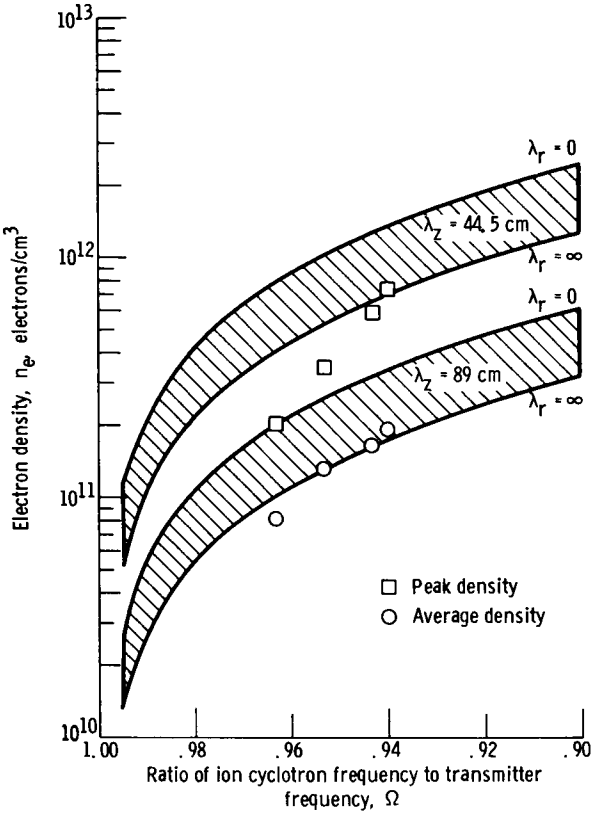

Figure 10. - Density at which resonance occurs as a function of Ω for the two major applied wavelengths. $\lambda_z^2 = \frac{4\pi^2}{An_e}\left[\frac{1-\Omega^2}{\Omega^2}\right]$ for $\lambda_r = 0$; $\lambda_z^2 = \frac{4\pi^2}{An_e}\left[\frac{1-\Omega}{\Omega^2}\right]$ for $\lambda_r = \infty$.